Improving aerosol distributions below clouds by assimilating satellite-retrieved cloud droplet number

Pablo E. Saide[a,1], Gregory R. Carmichael[a], Scott N. Spak[a], Patrick Minnis[b], and J. Kirk Ayers[c]

[a]Center for Global and Regional Environmental Research, University of Iowa, Iowa City, IA 52242; [b]NASA Langley Research Center, Hampton, VA 23681-0001; and [c]Science Systems and Applications, Inc., Hampton, VA 23666

Edited by Mark H. Thiemens, University of California San Diego, La Jolla, CA, and approved June 12, 2012 (received for review April 6, 2012)

Limitations in current capabilities to constrain aerosols adversely impact atmospheric simulations. Typically, aerosol burdens within models are constrained employing satellite aerosol optical properties, which are not available under cloudy conditions. Here we set the first steps to overcome the long-standing limitation that aerosols cannot be constrained using satellite remote sensing under cloudy conditions. We introduce a unique data assimilation method that uses cloud droplet number (N_d) retrievals to improve predicted below-cloud aerosol mass and number concentrations. The assimilation, which uses an adjoint aerosol activation parameterization, improves agreement with independent N_d observations and with in situ aerosol measurements below shallow cumulus clouds. The impacts of a single assimilation on aerosol and cloud forecasts extend beyond 24 h. Unlike previous methods, this technique can directly improve predictions of near-surface fine mode aerosols responsible for human health impacts and low-cloud radiative forcing. Better constrained aerosol distributions will help improve health effects studies, atmospheric emissions estimates, and air-quality, weather, and climate predictions.

air quality | indirect effect | weather prediction | stratiform cloud | microphysics

Ambient aerosols are important air pollutants with direct impacts on human health (1). They also play important roles in Earth's weather and climate systems through their direct (2), semi-direct (3), and indirect effects (4) on radiative transfer and clouds. Their role is dependent on their size, number, phase, and composition distributions, which vary significantly in space and time. There remain large uncertainties in predictions of aerosol distributions due to uncertainties in emission estimates and in chemical and physical processes associated with their formation and removal (5–9). These uncertainties in aerosol distributions lead to large uncertainties in weather and air-quality predictions and in estimates of health and climate-change impacts (10).

Constraining ambient aerosol distributions with current Earth-observing systems is a difficult task. The most common approach is to assimilate satellite retrievals of aerosol optical depth (AOD) (11, 12), a quantity that represents total aerosol mass and composition in the atmospheric column. The requirement of cloud-free conditions for a successful retrieval and the remaining challenges of relating AOD to aerosol mass, size, and composition limit the utility of AOD retrievals (by themselves) in constraining aerosol mass and composition (13, 14). These shortcomings are particularly true in regions of persistent marine stratocumulus, such as the southeast Pacific off the coast of Chile and Peru, where aerosol–cloud interactions are important to the energy balance (15), and limitations in current observing and modeling capabilities adversely impact regional and global weather and climate predictions (16). A typical MODIS AOD scene in this region (Fig. 1, *Upper Left*) shows that AOD provides essentially no useful information to constrain aerosol distributions when low clouds are present (Fig. S1).

Aerosols play an important role in cloud formation, acting as cloud condensation nuclei (CCN), and further affect cloud macro-and micro-physical properties such as albedo (17), drizzling capacity and lifetime (18), and cloud base and top heights (19), among others. Despite uncertainties (10) and challenges (20) in modeling aerosol–cloud interactions, recent studies have shown significant capabilities in predicting and explaining aerosol indirect effects in low cloud regimes (6, 7, 21). By building on this mechanistic understanding, observations of clouds may be used to infer aerosol physicochemical properties. This is done by using a unique data assimilation technique presented in *Methods* and described in depth in *SI Text*.

Results

The assimilation procedure is demonstrated for the case of the southeast Pacific's persistent stratocumulus deck, where in situ aircraft observations during the VOCALS-REx field experiment (22) provide independent accumulation mode aerosol mass and number concentrations (23) for verification. We predict meteorology and aerosol mass (M) and number (N) distributions at the regional scale with the WRF-Chem model (24, 25) configured for this area (6). Cloud optical depth and effective droplet radii retrieved from Terra MODerate-resolution Imaging Spectroradiometer (MODIS) and Geostationary Operational Environmental Satellite (GOES) imager data (26, 27) are used to compute observed N_d (28). We perform experiments utilizing these retrievals (see *SI Text*, Assimilation experiments). The impacts of assimilation of MODIS N_d on optimized modeled N_d, N, and aerosol sulfate mass concentration are shown in Fig. 1 for a day with an extensive and thick stratocumulus deck (Fig. 1, *Upper Right*, and Fig. S1), which is a typical condition in the region [e.g., daytime cloud fraction was between 70–90% during the VOCALS-REx period (7)]. The background modeled N_d (prior) resolves the longitudinal gradient in the observations defined by the indirect effects due to anthropogenic pollution (6) but generally overestimates coastal amounts and underestimates remote concentrations. The assimilation produces an improved a posteriori modeled N_d, as shown by a 30% fractional error reduction (*) and by the better resemblance of N_d assimilated fields compared to the observations (Fig. 1, first and second row). Assimilation increases (decreases) N and M in places where N_d is under (over) predicted (Fig. 1, third and fourth row), activating more (less) particles, thus reducing the error.

As the observation operator for this assimilation technique is a mixing-activation parameterization, the aerosols modified are those most active in the activation process; i.e., below cloud and accumulation mode aerosols. Coarse aerosols do participate

Author contributions: P.E.S., G.R.C., and S.N.S. designed research; P.E.S. performed research; P.E.S., G.R.C., S.N.S., P.M., and J.K.A. analyzed data; and P.E.S., G.R.C., S.N.S., P.M., and J.K.A. wrote the paper.

The authors declare no conflict of interest.

This article is a PNAS Direct Submission.

Freely available online through the PNAS open access option.

*Fractional error of 72% and 42% are obtained between GOES-10 retrieval and prior and assimilated fields respectively at one hour after assimilation (16Z).

[1]To whom correspondence should be addressed. E-mail: pablo-saide@uiowa.edu.

This article contains supporting information online at www.pnas.org/lookup/suppl/doi:10.1073/pnas.1205877109/-/DCSupplemental.

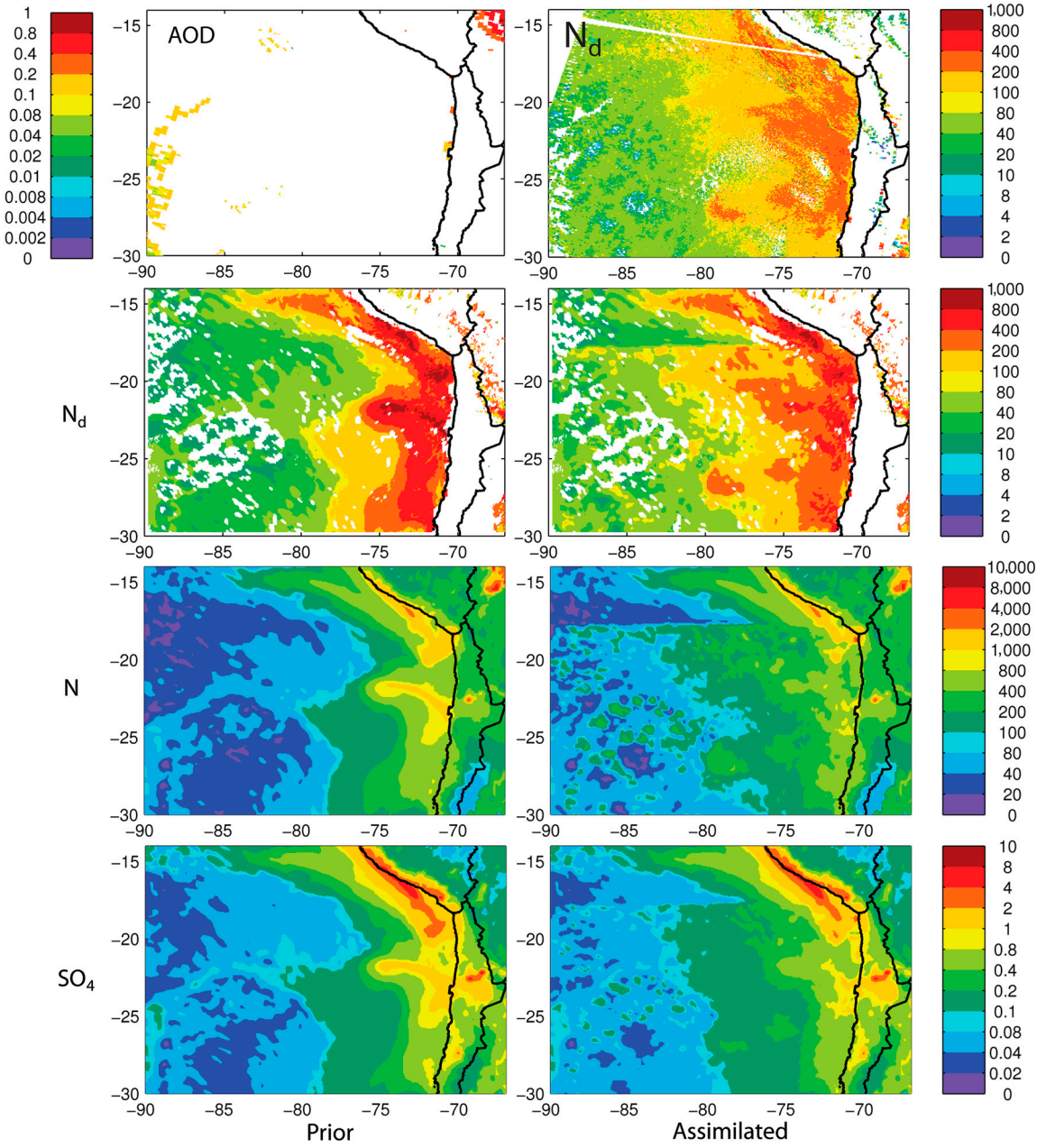


Fig. 1. Observed and model maps for the southeast Pacific and coastal Chile and Peru. (*Top Row*) MODIS AOD (*Left*) and N_d (*Right*, in #/cm^3) at October 16, 2008, at 15Z overpass. Second to fourth rows show prior (*Left*) and assimilated (*Right*) results for N_d, accumulation mode N (#/cm^3) and sub-micron sulfate concentrations (μg/m^3) one hour after assimilating MODIS N_d. See *SI Text*, Assimilation experiments, for further details.

in activation, but their sensitivities are low because their number concentrations are small. As vertical mixing is also considered, the aerosols modified are not only those in the layer immediately below clouds but also from lower near-surface layers. The vertical extent of the impact depends on the mixing state of the atmosphere below clouds. For cloud-capped marine boundary layers (as in the stratocumulus deck studied here), depending on the decoupling state (29) the aerosol constraint can extend to the sea surface. Thus, this technique can directly improve estimates of fine mode near-surface aerosol number, composition, and size. For instance, sulfate dominates the hygroscopic fine aerosol mass in the marine boundary layer (MBL) in this region throughout this study period (7) and therefore receives the most constraint from assimilation (Fig. 1, fourth row). Species during this period found mainly in the coarser size bins like nitrate and sea salt (7) are not impacted as much, and those found in the free troposphere above the cloud layer, such as biomass burning organic aerosol (23), are not affected by the assimilation.

The impact of assimilation on constraining aerosol distributions is evaluated in an experiment (see *SI Text*, Assimilation experiments, for further details) where GOES-10 N_d was assimilated at the time when a research flight was conducted that did a longitudinal in situ sampling of the cloud deck (Fig. 2, *Top*). The model prior underestimates offshore aerosol mass and number, which the assimilation corrects, reducing fractional biases by 25% and 33%, respectively. Similar assimilation experiments for two coastal pollution survey flights (Fig. 2, *Bottom*) improved statistical performance for below cloud aerosol mass and number, reducing fractional bias and error (30) and increasing spatiotemporal correlation in each case. The use of retrievals from geostationary satellites to constrain aerosols is an important advancement because it provides a significant improvement in temporal

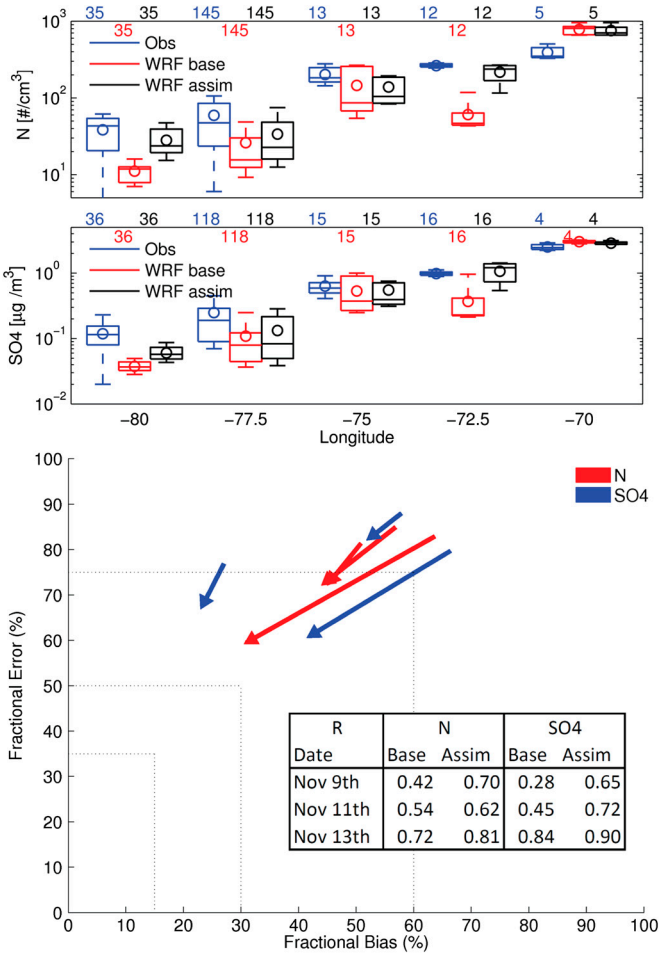


Fig. 2. Statistical comparison between modeled and in situ C-130 observations (23) of accumulation mode aerosol number concentration and fine sulfate mass. (*Top*) Longitudinal statistics as box and whisker plots for flight RF13 (November 13, 2008). Center solid lines indicate the median, circles represent the mean, boxes indicate upper and lower quartiles, and whiskers show the upper and lower deciles. Number of 1-min samples contributing to each longitudinal bin is indicated at the top. (*Bottom*) "Soccer goal" plot (30) showing bias and error improvements for flights RF11 (November 9, 2008), RF12 (November 11, 2008), and RF13. Each arrow represents *N* (red) and SO_4 (blue) for each flight, where the arrow tail and tip represent the base and assimilated model statistics, respectively. Arrows pointing toward (0, 0) indicate that assimilation improves both bias and error. The embedded table shows correlation (*R*) between models and observations. Model and measurements are below cloud. See *SI Text*, Assimilation experiments, for further details.

resolution (approximately 16 retrievals per day) compared to polar orbiting satellites that produce one retrieval per day.

An important feature of the cloud droplet number assimilation is that it results in a change in aerosol distribution, which can impact cloud predictions forward in time over the lifetime of the aerosols throughout the region of analysis (approximately 2 days in the MBL). To demonstrate this persistent effect of the constraint we assimilate a single retrieval of MODIS N_d and evaluate the forecast of N_d by comparing to independent hourly resolved GOES10 N_d retrievals (Fig. 3). One to five hour after assimilation (Fig. 3, first day) the magnitude and variability of forecast N_d over polluted and clean geographical regions are improved as seen by the enhancement in number and variability in the clean region and a decrease in mean and variability in the polluted zone, achieving a global 20–30% fractional error reduction. For the second day, model errors (6) and the transport of the aerosols out of the domain reduce the impact of the assimilated fields. However, the assimilation still has a positive impact on the forecasts that extends beyond 24 h. A snapshot 22 h after assimilation (Fig. 3, *Bottom*) shows features in the assimilation-predicted fields that resemble the observations and are not found in the prior: N_d enhancement over 100 #/cm^3 (near 20 °S, 85 °W) that can be traced to a plume present in the retrieval near 27 °S, 79 °W (Fig. 1); and an increase in cloud cover in the northwest of the domain that was missed in the background simulation. After 48 h, the assimilated aerosol has exited the regional model domain, and only small differences between background and assimilated fields remain. This lasting influence on cloud and aerosol properties could help overcome one of the main issues in contemporary cloud assimilation methods, where information gained in the analysis is attenuated within hours after initialization (31, 32).

Discussion

The technique presented here is designed for use with single-layer warm liquid cloud systems with vertically homogeneous N_d. These conditions represent low stratiform clouds, which persistently cover large regions around the world (e.g., stratocumulus decks off the west coasts of Africa and South and North America) and are pointed out as the main players in aerosol indirect forcing (33). While this first approach to N_d assimilation does not resolve the vertical N_d gradients and ice and graupel phases that arise from convection, convective clouds are often accompanied by or form from low clouds where this technique can be applied. Beyond regions of persistent low stratocumulus, single-layer liquid cloud conditions can also be identified in model calculations and matched with instantaneous cloud retrievals on a pixel-by-pixel basis and assimilated opportunistically throughout the world, whenever and wherever they occur. The application of this technique to other regions requires further evaluation of the N_d satellite retrieval calculation. Even though global estimates of N_d can be made (34), region-specific expressions evaluated using in situ measurements can help reduce uncertainty in the retrievals (28). In this sense, it is encouraging that for a given region, a single formula can be used across satellites and instruments (GOES imager, MODIS Aqua, and Terra) with excellent performance against N_d in situ data, remarkably better than for other retrieved cloud properties (28, 35). The activation parameterization and its assumptions represent another source of uncertainty (20), but again, comparisons with in situ and satellite measurements help better understand these limitations and their extent (6, 7). Expanded applications of this approach (e.g., aerosol retrieval and assimilation under multilayer, convective, and ice clouds) may be possible, but additional research and testing is required on both retrieval and modeling sides.

Potential applications for this technique are found throughout the atmospheric sciences and beyond. When incorporating aerosol indirect feedbacks on clouds in numerical weather prediction, better aerosol predictions can further improve MBL height and cloud heights, liquid and precipitable water, precipitation rates, cloud optical properties, and cloud lifetime (6). As aerosol influences on clouds have been shown to affect convective systems (36), lighting (37), tropical cyclones (38), and tornados (39), more accurate aerosol representation could also lead to better predictions for severe storms and hazards. In addition, better constrained fine and below-cloud aerosol distributions will help improve air quality predictions (12) and reduce uncertainties in assessments of health and climate impacts due to aerosols (11). The use of this technique is not limited to 3DVAR and may be used for sensitivity analysis (40) as well as being coupled to an adjoint of all model components for 4DVAR assimilation of aerosol state and evolution (12) or used in inverse modeling to better estimate emission sources. In this sense, important applications include improving highly uncertain estimates of oceanic organic emissions (8, 9) and constraining anthropogenic emissions such as those occurring upwind of persistent cloud regimes (e.g., central Chile and northern California) (6) and those

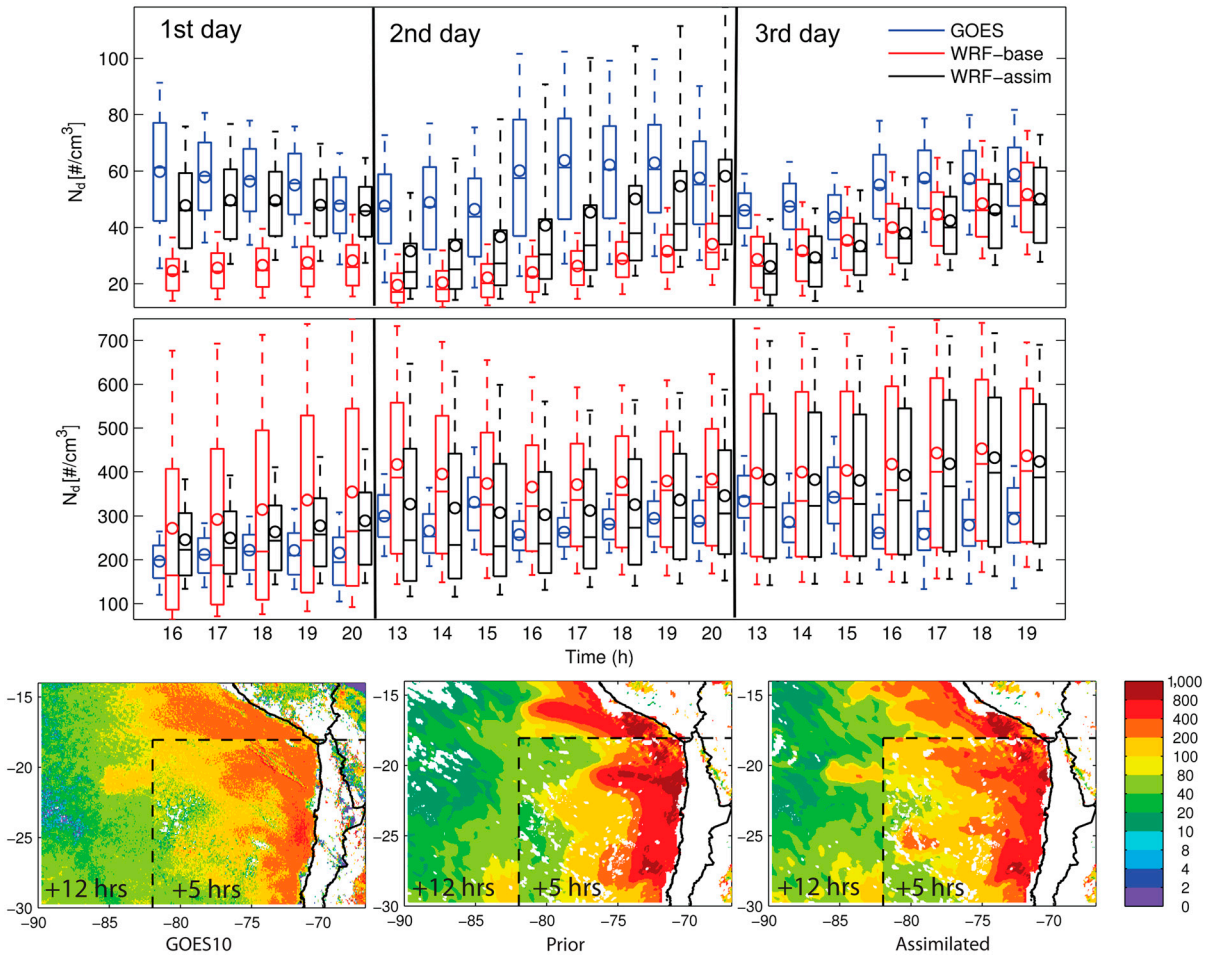


Fig. 3. (*Top*) Box and whisker plots as in Fig. 2 for time series of GOES10 and modeled N_d statistics on 5° × 5° areas centered at 20 °S,85 °W (*Top*) and 20 °S,75 °W (*Bottom*). In the assimilation, a single assimilation using MODIS N_d (Fig. 1, first row) is performed at 15 UTC on October 16 (first day), and then the model is run as a forecast for 72 h. Thick black vertical lines separate different consecutive days. (*Bottom*) Composite maps for GOES10 observations, model prior, and assimilated model N_d for October 16 at 20Z (southeast box, 5 h after assimilation) and October 17 at 13Z (remainder of the map to the west and north, 22 h after assimilation). See *SI Text*, Assimilation experiments, for further details.

emitted below clouds (e.g., ship emissions). These applications are not limited to persistent stratocumulus decks; similar aerosol feedbacks have been shown for other marine (41) and continental (42) shallow cumulus. Also, there is no limitation on aerosol composition distribution (sulfate dominates the case studied) as long as the aerosol properties participating in the activation process (e.g., hygroscopicity, solubility) are specified correctly. These applications are currently feasible given the availability of near real-time cloud retrievals (26).

The technique can be combined with AOD assimilation to constrain aerosol distributions for mass, number, composition, and optical properties over a broader range of conditions, as AOD and N_d assimilation are complementary, employing observations that do not coexist (e.g., there is no AOD retrieval when there are clouds and vice-versa). Using these retrievals together enables the observing system (satellites retrievals + model simulations) to "see aerosols" for a larger number of pixels in a scene, even under cloudy conditions.

Methods

We propose a unique data assimilation technique (Fig. S2) to improve aerosol mass (*M*) and number (*N*) distributions from satellite retrievals of cloud droplet number (N_d) and demonstrate it for a stratocumulus application, where these remote sensing products have been shown to accurately represent in situ N_d observations (28, 35, 43). The forward model includes a vertical mixing-activation parameterization used to predict N_d from meteorological conditions and initial *M* (composition/size/phase resolved), *N* (size/phase resolved), and N_d distributions. Sensitivities of predicted N_d derived with respect to these input variables are computed efficiently using the adjoint of the mixing-activation parameterization. These sensitivities are then utilized in a formal data assimilation framework to find the optimal model state that best fits the N_d observations considering confidence in both the observations and the initial conditions. We chose to optimize for initial *N* only because it has been shown to be the most important contributor to N_d sensitivities over other variables such as vertical velocity and aerosol composition for most conditions (20, 44), especially over oceans (40, 45, 46). This is accomplished through three-dimensional variational (3DVAR) data assimilation with a log-normal cost function and five-dimensional (3D in space + size + phase) *N* covariances. Assimilation yields size-, phase-, and space-resolved correction factors for *N*, which are further applied to each *M* composition bin (assuming the internal composition of each size/phase bin remains the same), resulting in an updated aerosol mass for each compound as well. Further details on the technique can be found in *SI Text*, Observations, Observation operator (Forward and Adjoint Models), and Assimilation method.

ACKNOWLEDGMENTS. We would like to acknowledge insightful comments of Marc Bocquet, Elliott Campbell, and two anonymous reviewers. We also thank all VOCALS-REx participants, specially Antony Clarke, Steve Howell and Lindsey Shank for AMS and PCASP data. This work was carried out with the aid of National Science Foundation (NSF) Grant 0748012, Fulbright-CONICYT (Comisión Nacional de Investigación Científica y Tecnológica de Chile) scholarship number 15093810, NASA grants NNX08AL05G and NNX11AI52G, the NASA Modeling, Analysis and Prediction (MAP) Program, and the Department of Energy (DoE) Atmospheric System Research (ASR) Program. This research was supported in part through computational resources provided by The University of Iowa, Iowa City, Iowa.

1. Pope CA, Young B, Dockery D (2006) Health effects of fine particulate air pollution: Lines that connect. *J Air Waste Manag Assoc* 56:709–742.
2. Bellouin N, Boucher O, Haywood J, Reddy MS (2005) Global estimate of aerosol direct radiative forcing from satellite measurements. *Nature* 438:1138–1141.
3. Ackerman AS, et al. (2000) Reduction of tropical cloudiness by soot. *Science* 288:1042–1047.
4. Lohmann U, Feichter J (2005) Global indirect aerosol effects: A review. *Atmos Chem Phys* 5:715–737.
5. Mebust MR, Eder BK, Binkowski FS, Roselle SJ (2003) Models-3 community multiscale air quality (CMAQ) model aerosol component 2. Model evaluation. *J Geophys Res* 108:4184–4201.
6. Saide PE, et al. (2012) Evaluating WRF-Chem aerosol indirect effects in southeast Pacific marine stratocumulus during VOCALS-REx. *Atmos Chem Phys* 12:3045–3064.
7. Yang Q, et al. (2011) Assessing regional scale predictions of aerosols, marine stratocumulus, and their interactions during VOCALS-REx using WRF-Chem. *Atmos Chem Phys* 11:11951–11975.
8. Heald CL, Ridley DA, Kreidenweis SM, Drury EE (2010) Satellite observations cap the atmospheric organic aerosol budget. *Geophys Res Lett* 37:L24808.
9. Meskhidze N, et al. (2011) Global distribution and climate forcing of marine organic aerosol: 1. Model improvements and evaluation. *Atmos Chem Phys* 11:11689–11705.
10. Solomon S, et al. (2007) *Climate change 2007: The physical science basis: Contribution of Working Group I to the Fourth Assessment Report of the Intergovernmental Panel on Climate Change* (Cambridge Univ Press, Cambridge, United Kingdom).
11. Carmichael GR, et al. (2009) Asian aerosols: Current and year 2030 distributions and implications to human health and regional climate change. *Environ Sci Technol* 43:5811–5817.
12. Benedetti A, et al. (2009) Aerosol analysis and forecast in the European Centre for Medium-Range Weather Forecasts Integrated Forecast System: 2. Data assimilation. *J Geophys Res* 114:D13205.
13. Kahn RA, et al. (2007) Satellite-derived aerosol optical depth over dark water from MISR and MODIS: Comparisons with AERONET and implications for climatological studies. *J Geophys Res* 112:D18205.
14. Redemann J, et al. (2006) Assessment of MODIS-derived visible and near-IR aerosol optical properties and their spatial variability in the presence of mineral dust. *Geophys Res Lett* 33:L18814.
15. George R, Wood R (2010) Subseasonal variability of low cloud radiative properties over the southeast Pacific Ocean. *Atmos Chem Phys* 10:4047–4063.
16. Wyant MC, et al. (2010) The PreVOCA experiment: Modeling the lower troposphere in the Southeast Pacific. *Atmos Chem Phys* 10:4757–4774.
17. Twomey S (1991) Aerosols, clouds and radiation. *Atmos Environ* 25:2435–2442.
18. Albrecht BA (1989) Aerosols, cloud microphysics, and fractional cloudiness. *Science* 245:1227–1230.
19. Pincus R, Baker MB (1994) Effect of precipitation on the albedo susceptibility of clouds in the marine boundary layer. *Nature* 372:250–252.
20. McFiggans G, et al. (2006) The effect of physical and chemical aerosol properties on warm cloud droplet activation. *Atmos Chem Phys* 6:2593–2649.
21. Kazil J, et al. (2011) Modeling chemical and aerosol processes in the transition from closed to open cells during VOCALS-REx. *Atmos Chem Phys* 11:7491–7514.
22. Wood R, et al. (2011) The VAMOS Ocean-Cloud-Atmosphere-Land Study Regional Experiment (VOCALS-REx): Goals, platforms, and field operations. *Atmos Chem Phys* 11:627–654.
23. Allen G, et al. (2011) South East Pacific atmospheric composition and variability sampled along 20 °S during VOCALS-REx. *Atmos Chem Phys* 11:5237–5262.
24. Grell GA, et al. (2005) Fully coupled "online" chemistry within the WRF model. *Atmos Environ* 39:6957–6975.
25. Skamarock WC, et al. (2008) A description of the Advanced Research WRF version 3. *NCAR Tech. Note NCAR/TN-475+STR*113, Available online at http://www.mmm.ucar.edu/wrf/users/docs/arw_v3.pdf.
26. Minnis P, et al. (2008) Near-real time cloud retrievals from operational and research meteorological satellites. *Proc SPIE* 7107:710703–710710.
27. King MD, et al. (2006) Collection 005 change summary for the MODIS cloud optical property (06_OD) algorithm. *MODIS Atmosphere* p 8.
28. Painemal D, Zuidema P (2011) Assessment of MODIS cloud effective radius and optical thickness retrievals over the southeast Pacific with VOCALS-REx in situ measurements. *J Geophys Res* 116:D24206.
29. Jones CR, Bretherton CS, Leon D (2011) Coupled vs. decoupled boundary layers in VOCALS-REx. *Atmos Chem Phys* 11:7143–7153.
30. Morris RE, et al. (2005) Preliminary evaluation of the Community Multiscale Air Quality model for 2002 over the southeastern United States. *J Air Waste Manag Assoc* 55:1694–1708.
31. Bauer P, Ohring G, Kummerow C, Auligne T (2011) Assimilating satellite observations of clouds and precipitation into NWP models. *Bull Am Meteorol Soc* 92:25–28.
32. Auligné T, et al. (2011) Toward a new cloud analysis and prediction system. *Bull Am Meteorol Soc* 92:207–210.
33. Kogan ZN, Kogan YL, Lilly DK (1996) Evaluation of sulfate aerosols indirect effect in marine stratocumulus clouds using observation-derived cloud climatology. *Geophys Res Lett* 23:1937–1940.
34. Bennartz R (2007) Global assessment of marine boundary layer cloud droplet number concentration from satellite. *J Geophys Res* 112:D02201.
35. Painemal D, Minnis P, Ayers JK, O'Neill L (2012) GOES-10 microphysical retrievals in marine warm clouds: Multi-instrument validation and daytime cycle over the southeast Pacific. *J Geophys Res*, in press.
36. Koren I, Kaufman YJ, Rosenfeld D, Remer LA, Rudich Y (2005) Aerosol invigoration and restructuring of Atlantic convective clouds. *Geophys Res Lett* 32:L14828.
37. Yuan T, Remer LA, Pickering KE, Yu H (2011) Observational evidence of aerosol enhancement of lightning activity and convective invigoration. *Geophys Res Lett* 38:L04701.
38. Rosenfeld D, Clavner M, Nirel R (2011) Pollution and dust aerosols modulating tropical cyclones intensities. *Atmos Res* 102:66–76.
39. Rosenfeld D, Bell TL (2011) Why do tornados and hailstorms rest on weekends? *J Geophys Res* 116:20211–20224.
40. Karydis VA, Capps SL, Russell AG, Nenes A (2012) Adjoint sensitivity of global cloud droplet number to aerosol and dynamical parameters. *Atmos Chem Phys Discuss* 12:12081–12117.
41. Yuan T, Remer LA, Yu H (2011) Microphysical, macrophysical and radiative signatures of volcanic aerosols in trade wind cumulus observed by the A-Train. *Atmos Chem Phys* 11:7119–7132.
42. Berg LK, Berkowitz CM, Barnard JC, Senum G, Springston SR (2011) Observations of the first aerosol indirect effect in shallow cumuli. *Geophys Res Lett* 38:L03809.
43. Bretherton C, et al. (2010) Southeast Pacific stratocumulus clouds, precipitation and boundary layer structure sampled along 20 °S during VOCALS-REx. *Atmos Chem Phys* 10:10639–10654.
44. Feingold G (2003) Modeling of the first indirect effect: Analysis of measurement requirements. *Geophys Res Lett* 30:1997–2000.
45. Quaas J, Boucher O, Bellouin N, Kinne S (2008) Satellite-based estimate of the direct and indirect aerosol climate forcing. *J Geophys Res* 113:D05204.
46. Hegg DA, Covert DS, Jonsson HH, Woods RK (2012) A simple relationship between cloud drop number concentration and precursor aerosol concentration for the regions of Earth's large marine stratocumulus decks. *Atmos Chem Phys* 12:1229–1238.